



Discovery of drug lead compounds for Anti-Alzheimer's disease on the basis of synaptic plasticity

Heyu Wang, Quan Tang, Yanyu Xue, Xiaoqian Gao, Yan Zhang*

College of Life and Environmental Sciences, Minzu University of China, Beijing 100081, China

ARTICLE INFO

Keywords:

Alzheimer's disease
Synaptic plasticity
Natural active compounds
Molecular docking
Pharmacological experiment

ABSTRACT

Alzheimer's disease (AD) is a progressive neurodegenerative disease commonly seen in the middle-aged and the elder. Its clinical presentations are mainly memory impairment and cognitive impairment. Its cardinal pathological features are the deposition of extracellular Amyloid- β ($A\beta$), intracellular neurofibrillary tangles and synaptic dysfunction. The etiology of AD is complex and the pathogenesis remains unclear. Having AD would lead to awful living experience of it's patients, which may be a burden to the patient even to the public health care system. However, there are no certain cure for AD. Thus it's significant for both medical value and social meaning to find the way to cure or prevent AD and to research on the pathogenesis of AD. In this work, the molecular docking technology, pharmacokinetic analysis and pharmacological experiments were employed to analyse the natural active compounds and the mechanisms against AD based on the synaptic plasticity. A total of seven target proteins related to the synaptic plasticity and 44 natural active compounds with potential to enhance the synaptic plasticity were obtained through a literature review and network pharmacological analysis. Computer-Aided Drug Design (CADD) method was used to dock the anti-AD key target proteins with the 44 compounds. The compounds with good binding effect were screened. Three anti-AD active compounds based on the synaptic plasticity were obtained, including *Curcumin*, *Withaferin A* and *Withanolide A*. In addition, pharmacological experiments were carried out on *Withaferin A* and *Withanolide A* based on its good docking results. The experimental results showed that *Withaferin A* has good anti-AD potential and great potential to enhance synaptic plasticity. The anti-AD effect can be achieved through a multi-target synergistic mechanism.

1. Introduction

Alzheimer's disease is a progressive neurological dementia that causes impairments in cognition and behaviour [1]. It is estimated that there are 50 million AD patients worldwide [2]. The disease is associated with synaptic dysfunction, amyloid plaques deposition, neurofibrillary tangles (NFTs) caused by phosphorylated tau protein (p-tau) [3], synapse and neuronal loss [4] and significant reductions in choline acetyltransferase (ChAT) and acetylcholine (ACh) [5]. A synapse is a specific connector that transmits information between neurons, between neurons and muscle cells or between neurons and glands by neurotransmitters [6]. The connection strength of synapses can be adjusted. This characteristic is called synaptic plasticity [7]. Synaptic plasticity is considered to be the basis of brain learning and memory [8]. There is a strong correlation between the decrease of hippocampal area synapses and the decline of

* Corresponding author.

E-mail address: zhangyan@muc.edu.cn (Y. Zhang).

<https://doi.org/10.1016/j.heliyon.2023.e18396>

Received 1 December 2022; Received in revised form 12 July 2023; Accepted 17 July 2023

Available online 17 July 2023

2405-8440/© 2023 The Authors. Published by Elsevier Ltd. This is an open access article under the CC BY-NC-ND license (<http://creativecommons.org/licenses/by-nc-nd/4.0/>).

cognition in AD patients [9,10]. However, the changes of synapses and proteins related synapse plasticity occur earlier than the decrease in synapses [11]. Therefore, proteins related synapse plasticity may be potential targets of AD, especially the synergism of various protein targets.

The pathogenesis of AD is extremely complex and is still unclear. With the continuous exploration of AD, a series of hypotheses was formed, mainly including A β abnormal deposition hypothesis, Tau abnormal phosphorylation hypothesis, cholinergic hypothesis, oxidative stress hypothesis, brain-gut axis hypothesis, neuron-synapse loss hypothesis, etc. All these mechanisms have an important impact on the pathogenesis and the treatment of AD. Oxidative stress means that the reactive oxygen species (ROS) exceeds the normal antioxidant level, the body loses the balance of the redox response, and then causing cell damage and apoptosis [12]. Impaired mitochondrial function and the imbalance of the redox reaction in the body may cause excessive ROS, which will directly affect the transmission of the neurotransmitters and synaptic function, aggravate the damage of mitochondrial function, and accelerate the generation of A β [13]. A large number of studies have shown that the level of ROS has a correlation with the pathogenesis of AD, so we can treat AD by regulating the ROS level and reducing the oxidative stress damage [14].

Medicinal plants are being increasingly evaluated in studies of AD due to their lower toxicity and fewer side effects, low cost and good curative effect. A large number of pharmacological experiments have shown that medicinal plants and their active ingredients have the potential to treat AD, including the active ingredients triphlorolide in Celastraceae *Tripterygium wilfordii* [15], pratensein in Leguminosae *Trifolium pratense* [16], xanthoceraside in Sapindaceae *Xanthoceras sorbifolia* [17], and platycodin D in Campanulaceae *Platycodon grandiflorum* [18]. Some active ingredients of medicinal plants have been used in clinical treatments, such as Galanthamine in *Lycoris* plants [18], Huperzine A in *Huperzia serrata* [19,20], and Salidroside in *Rhodiola rosea* L.

Computer-Aided Drug Design (CADD) is a drug design method based on the basic principle of theoretical chemistry. It simulates the interactions between drugs and receptor molecules to analyse the internal relationships between drug structure and biological activity and rationally designs new structures for lead compounds. The use of computational methods can increase efficiency and reduce costs in the drug discovery process, making these approaches the best alternatives in the discovery of drug lead compounds.

In this study, 44 natural active compounds were screened on the basis of 22 proteins related to synaptic plasticity. Pharmacological experiments were carried out to verify their effects.

2. Materials and methods

2.1. Preparation of receptors and ligands

In this study, 22 proteins related to synaptic plasticity were analyzed and selected as the research basis (Table 1). We used the STRING database (<https://string-db.org>) to obtain protein interaction data and Cytoscape 3.6.1 software to construct the protein interaction network. Seven key anti-AD target proteins were selected according to the topological parameters (Table 2). At the same time, we used the STRING database to carry out GO function and KEGG pathway enrichment analyses [21].

In this study, 44 natural active compounds with the potential to enhance synaptic plasticity were collected and sorted as the research basis (Table 3).

Table 1
Proteins related to synaptic plasticity.

No.	Protein	Gene	UniProt ID
1	Glutamate receptor ionotropic, NMDA 2 B	GRIN2B	Q13224
2	Leukocyte immunoglobulin-like receptor subfamily B member 2	LILRB2	Q8N423
3	Calcium/calmodulin-dependent protein kinase type II subunit gamma	CAMK2G	Q13555
4	Disks large homolog 4	DLG4	P78352
5	Cyclic AMP-responsive element-binding protein 1	CREB1	P16220
6	PRKCA-binding protein	PICK1	Q9NRD5
7	Glutamate receptor 1	GRIA1	P42261
8	Prolow-density lipoprotein receptor-related protein 1	LRP1	Q07954
9	Brain-derived neurotrophic factor	BDNF	P23560
10	Beta-nerve growth factor	NGF	P01138
11	BDNF/NT-3 growth factors receptor	NTRK2	Q16620
12	Hepatocyte growth factor receptor	MET	P08581
13	Beta-2 adrenergic receptor	ADRB2	P07550
14	Glutamate receptor ionotropic, kainate 2	GRIK2	Q13002
15	Reticulon-4 receptor	RTN4R	Q9BZR6
16	Synapsin-1	SYN1	P17600
17	Neuromodulin	GAP43	P17677
18	Amyloid-beta precursor protein	APP	P05067
19	5-hydroxytryptamine receptor 1 A	HTR1A	P08908
20	Glycogen synthase kinase-3 beta	GSK3B	P49841
21	Tumour necrosis factor receptor superfamily member 16	NGFR	P08138
22	Protein kinase C epsilon type	PRKCE	Q02156

Table 2

Degree, betweenness and closeness and their relationships with the average targets.

ID	Target protein	PDB ID	Degree	Betweenness	Closeness
1	BDNF	1bnd	16	0.12829353	0.833333
2	GRIN2B	5 EWJ	15	0.06403288	0.8
3	GRIA1	–	15	0.08528601	0.8
4	NGF	1SG1	14	0.07305543	0.769231
5	DLG4	6SPZ	14	0.05326847	0.769231
6	APP	2WK3	14	0.13059561	0.769231
7	CREB1	2LXT	14	0.05170426	0.769231

Note: The protein structure of the GRIA1 protein was not found in the PDB database, so no PDB ID is available. For its data, we obtained the consent from the Journal of the Minzu University of China (Natural Sciences Edition) [21].

Table 3

Natural active compounds with the potential to enhance synaptic plasticity.

No.	Compound	PubChem ID	Plant source	Reference
1	Paeoniflorin	442,534	<i>Paeonia lactiflora</i> Pall	[22]
2	Albiflorin	51,346,141	<i>Paeonia lactiflora</i> Pall	[23]
3	Tripchlorolide	159,588	<i>Tripterygium wilfordii</i>	[18]
4	Huperzine A	854,026	<i>Huperzia serrata</i>	[24]
5	Curcumin	969,516	<i>Curcuma longa</i>	[25]
6	Dihydromyricetin	161,557	<i>Ampelopsis megalophylla</i>	[26]
7	Malvidin 3-O-glucoside	443,652	<i>Vitis vinifera</i>	[27]
8	Andrographolide	5,318,517	<i>Andrographis paniculata</i>	[28]
9	Puerarin	5,281,807	<i>Pueraria montana</i>	[29]
10	Pratensein	5,281,803	<i>Trifolium pratense</i>	[16]
11	Chrysin	5,281,607	<i>Oroxylum indicum</i>	[30]
12	Paeonol	11,092	<i>Paeonia suffruticosa</i>	[31]
13	Resveratrol	445,154	<i>Reynoutria japonica</i>	[32]
14	Flavanol	253,959	<i>Cassia nomame</i>	[25]
15	Cannabidiol	644,019	<i>Cannabis sativa</i>	[33]
16	Luteolin	5,280,445	<i>Reseda odorata</i>	[34]
17	Gastrodin	115,067	<i>Gastrodia elata</i>	[32]
18	Hesperidin	10,621	<i>Hemerocallis citrina</i>	[32]
19	Macranthol	180,210	<i>Illicium dunnianum</i>	[32]
20	Rosmarinic acid	5,281,792	<i>Perilla frutescens</i>	[32]
21	Catalpol	91,520	<i>Rehmannia glutinosa</i>	[32]
22	Baicalin	5,281,605	<i>Scutellaria baicalensis</i>	[32]
23	Tetrandrine	73,078	<i>Stephania tetrandra</i>	[32]
24	Tenuigenin	12,442,762	<i>Polygala tenuifolia</i>	[35]
25	Icariin	5,318,997	<i>Epimedium brevicornu</i>	[36]
26	Apocynin A	9,804,654	<i>Apocynum venetum</i>	[37]
27	Platycodin D	162,859	<i>Platycodon grandiflorus</i>	[18]
28	Timosaponin A3	15,953,793	<i>Anemarrhena asphodeloides</i>	[38]
29	Xanthoceraside	102,336,202	<i>Xanthoceras sorbifolium</i>	[17]
30	Dactylorhin B	24,039,355	<i>Dactylorhiza viridis</i>	[39]
31	Ginsenoside rb1	9,898,279	<i>Panax ginseng</i>	[40]
32	ginsenoside-Rg1	441,923	<i>Panax ginseng</i>	[40]
33	Ginsenoside Rg2	21,599,924	<i>Panax ginseng</i>	[41]
34	Bilobalide	73,581	<i>Ginkgo biloba</i>	[42]
35	Hyperforin	441,298	<i>Hypericum perforatum</i>	[43]
36	Quercetin	5,280,343	<i>Styphnolobium japonicum</i>	[44]
37	Taxifolin	439,533	<i>Larix gmelinii</i>	[45]
38	Oleanolic acid	10,494	<i>Ligustrum lucidum</i>	[46]
39	Withaferin A	265,237	<i>Withania somnifera</i>	[47]
40	Withanolide A	11,294,368	<i>Withania somnifera</i>	[47]
41	Isocoumarins	68,108	<i>Itadaphne caudata</i>	[48]
42	Cotinine	854,019	<i>Nicotiana tabacum</i>	[49]
43	Betaine	247	<i>Lycium chinense</i>	[50]
44	Dihydrocaffeic acid	348,154	<i>Eucommia ulmoides</i>	[27]

2.2. Molecular docking

Seven key target proteins were docked with the 44 compounds. The corresponding 3D structures of target proteins in the docking study were downloaded from the Protein Data Bank (PDB, <http://www.Rcsb.org>) and the UniProt database (<https://www.uniprot.org>); The ligand compound structures were downloaded from PubChem (<https://pubchem.ncbi.nlm.nih.gov>). We defined the intrinsic ligand's centric position of the receptor protein crystal structure in the PDB and UniProt database as our docking site.

Discovery Studio 2019 (DS 2019) software was used for molecular docking and pharmacokinetic analyses. First, the ligands and receptors were optimized by DS 2019. The receptor proteins were pretreated with the “Macromolecules | Prepare protein” module, and the ligand compounds were pretreated with the “Small Molecule | Prepare Ligands” module. Next, the “Receptor-Ligand Interactions | Dock Ligands” function of CDOCKER was used for semiflexible molecular docking. “Receptor-Ligand Interactions|Flexible Docking” was used to conduct fully flexible molecular docking on the active compounds screened by semiflexible docking. The evaluation indices of the two molecular docking approaches were based on the CDOCKER_INTERACTION_ENERGY (CIE/ $\text{kJ}\cdot\text{mol}^{-1}$) (interaction energy between ligand and receptor). The lower the CIE, the less energy was required for the molecular docking and the more stable the docking system.

2.3. Pharmacokinetic analysis

DS 2019 was used to predict the absorption, distribution, metabolism, excretion and toxicity (ADMET) properties of potential anti-AD active compounds. First, compounds screened by fully flexible docking were introduced into DS 2019. Then, “Small Molecules” was expanded, “Calculate Molecular Properties” was selected, and “ADMET Descriptors” was chosen to set the parameters. The “Input Ligands” parameter group selected all active compound molecules, and the “ADMET Descriptors” parameter group selected all ADMET properties. Finally, the analysis was run.

2.4. Pharmacological experiment

2.4.1. Animals

Sprague-Dawley (SD) suckling rats were provided by Vital River Laboratory (Beijing, China, license number SCXK (Beijing) 2011–0012). All animal experiments were performed in accordance with the Guidelines for Care and Use of Laboratory Animals of Beijing Municipality and approved by Animal Ethics Committee of Minzu University of China.

2.4.2. Primary culture and AD model establishment of hippocampal neurons

The hippocampi were dissected from SD suckling rat in aseptic conditions, mechanically dissociated and digested with 0.25% trypsin (#T1350-100, Solarbio) for 25 min at 37 °C. Digestion was terminated with DMEM/F12 medium (#SH30023-01 B, Hyclone) supplemented with 10% fetal bovine serum and 1% penicillin-streptomycin (#15140–122, Gibco). Then, cells were collected by centrifugation at 1100 rpm for 3 min and suspended at a density of 1×10^5 cells/mL, plated on poly-D-lysine-coated 24-well plates, cultured in a humidified atmosphere of 5% CO₂ in air at 37 °C. The DMEM was replaced with neurobasal medium (#21103–049, Gibco) containing B27 supplement (#17504–044, Gibco), which was replaced every two days and cultured for 6–8 days.

The Alzheimer’s disease (AD) hippocampal neuron model was established by H₂O₂ damage. After 7 days of cell culture, cells were injured with H₂O₂ solution at different concentrations (100 μM , 150 μM , 200 μM , 250 μM , and 300 μM) for 24 h. An MTT assay was performed to determine the H₂O₂ concentration when the injury rate of hippocampal neurons reached 50%–60%, and the injury model was established.

2.4.3. cell viability assay

To study the effect of *Withaferin A* and *Withanolide An* on cell viability, we used 4,5-dimethyl-2-thiazolyl)-2,5-diphenyl-2-H-tetrazolium bromide (MTT) assay. MTT is a yellow tetrazolium salt that is reduced to purple formazan by active cells. To a 96-well plate, 10 μl MTT (#M2128, Sigma) and 90 μl DMEM medium were added. The DMEM was supplemented with 10% fetal bovine serum and 1% penicillin-streptomycin. After 4 h at 37 °C and 5% CO₂, the medium was replaced with 110 μl formazan solution. The absorbance of the dissolved formazan was measured at 490 nm using an enzyme-linked immunoassay. In this study, after 7 days’ cell culture of hippocampal neuron, the control group cells were pre-incubated with neurobasal medium; The AD model cells were pre-incubated with neurobasal medium containing 150 μM H₂O₂; The experimental group were pre-incubated with neurobasal medium containing 150 μM H₂O₂ and various concentrations of *Withaferin A* (0.01, 0.1, 0.5, and 1 μM) and *Withanolide A* (0.1, 1, 5, and 10 $\mu\text{g}/\text{ml}$).

2.4.4. Real-time fluorescent quantitative PCR

Real-time fluorescent quantitative PCR included RNA extraction, cDNA synthesis and real-time quantitative PCR amplification reactions. Frozen samples were transferred to EP tubes with 1 ml Trizol (#R1100, Solarbio) on ice. Total RNA was isolated from the hippocampal neurons using an RNAeasy kit (#ZP404, Zoman). RNA quantity and quality were determined by optical absorbance and the A260/A280 ratio using a Quikdrop nucleic acid protein concentration tester. Then, total RNA, RT Enzyme Mix, RT Reaction Mix and ddH₂O were mixed in a volume ratio of 4:3:7:3. To synthesize cDNA, the samples were incubated at 45 °C for 15 min, and the

Table 4
Primer sequences.

Target	Forward Primer	Reverse Primer
ERK	GAAGCCGTGGGAACCAAC	CGCATACGGTTTCAGCTTCG
CREB	GACGGAGGAGCTGTACCAC	AATCTGTGGCTGGGCTTGAA
BDNF	AATAATGTCTGACCCAGTGCC	CCCGGTCTCATCAAAGCCTG
TrkB	TCCCCACTTGATTCTGACCC	GAGGGTGAGGGAATGGACAA

reaction was inactivated at 85 °C for 5 min. The primer sequences are given in Table 4. Next, the reactions were mixed as shown in Table 5, placed in real-time fluorescence quantitative PCR instrument, and the cycle was run with the following parameters: pre-denaturation at 95 °C for 10 min, denaturation at 95 °C for 20 s, annealing at 58 °C for 30 s, 45 cycles. The dissolution curve was 95 °C for 10 s; 65 °C for 60 s; 97 °C for 1 s.

2.5. Statistical analysis

All results obtained were processed using Microsoft Excel and Graph Pad Prism 8 statistical analysis software. The two tailed *t*-test method was used for data comparisons between the two groups. One-way ANOVA was used to calculate data significance between more than two groups. The Bonferroni post hoc test was then performed.

3. Results

3.1. CDOCKER and flexible docking

A total of 32 compounds with high binding stability to 7 key target proteins were screened from 44 compounds through CDOCKER calculation, as shown in Table 6. The other 12 compounds were abandoned. The CDOCKER results showed that the target proteins BDNF, GRIN2B, GRIA1, NGF and DLG combined well with a variety of compounds. None of the 44 compounds could be bound to the target protein APP. Only compound 5 could be bound to the target protein CREB1, and the interaction energy (CIE value) was $-35.9604 \text{ kJ mol}^{-1}$. Compound 18 could be bound to the GRIN2B, GRIA1, DLG4, BDNF target proteins respectively, with good binding. Therefore, Compound 18 had multi-target potential. The interaction energy between Compound 30 and GRIA1 was the lowest, and the CIE value is $-89.769 \text{ kJ mol}^{-1}$, which was much lower than other docking results with GRIA1, indicating that Compound 30 and GRIA1 protein had the best binding in CDOCKER.

Flexible docking was conducted on the 32 compounds on the basis of the CDOCKER results. A total of 12 compounds were selected from the 32 compounds, including Compounds 3, 4, 5, 10, 11, 12, 13, 14, 22, 39, 40 and 44 (the specific names of the compounds are provided in Table 3). The results are shown in Table 7. Among them, Compounds 5, 39 and 40 not only had low interaction energy with key target proteins but also showed multi-target potential, indicating that they can stably bind to multiple key target proteins, such as GRIN2B and GRIA1. The optimum conformation binding modes of Compounds 5, 39 and 40 with GRIN2B and GRIA1 are shown in Figs. 1–3.

From Fig. 1, we can see the benzene ring of Compound 5 forms hydrophobic interactions with amino acid residue P492 of the target protein GRIN2B. At the same time, it forms seven hydrogen bond interactions with amino acid residue Y464, T494, R499, S668, T669, and E719 of the target protein GRIN2B. The skeleton between the two ketone groups forms an electrostatic interaction with R499 (Fig. 1A). As shown in Fig. 1B, Compound 5 also forms multiple types of interactions with amino acid residues of the target protein GRIA1, including electrostatic and hydrophobic interactions with Y109. Meanwhile, the phenyl ring is bound to L135, F176, and P177 through hydrophobic interactions. In addition, Compound 5 forms two hydrogen bonds with E106 and R115. According to its interaction energy (Table 7) and binding mode (Fig. 1), the CIE of Compound 5 and GRIN2B was $-57.3884 \text{ kJ mol}^{-1}$, indicating that it had a better binding effect with target protein GRIN2B and that the docking system was more stable.

Compound 39 forms hydrophobic interactions with amino acid residues Y464, A466, L664, A666, and L718 and 5 hydrogen bond interactions with amino acid residues K463, L664, T669, and L717 of the target protein GRIN2B (Fig. 2A). Fig. 2B shows Compound 39 forms multiple hydrophobic interactions with amino acid residues A107, Y109, I133, L135 of the target protein GRIA1, an electrostatic interaction with Q110 and a hydrogen bond interaction with S132. According to its interaction energy (Table 7) and binding mode (Fig. 2), Compound 39 had a better binding effect with target protein GRIN2B, and the docking system was more stable.

Fig. 3 shows Compound 40 interaction to GRIN2B, forming hydrophobic interactions with amino acid residues Y464, A466, and M722 and two hydrogen bond interactions with E416 and Y464 (Fig. 3A). Hydrophobic interactions between Compound 40 and the amino acid residues of the target protein GRIA1 were the most abundant. The amino acid residues A107, Y109, I133, M134, L135, and P177 of the target protein GRIA1 all bound to Compound 40 in the form of hydrophobic interactions. Compound 40 also forms 3 hydrogen bond interactions with E106, F113, and T233 (Fig. 3B). According to its interaction energy (Table 7) and binding mode (Fig. 3), the interactions between Compound 40 and the target protein GRIA1 were more abundant, indicating that Compound 40 bound more easily to GRIN2B and that the binding system was more stable.

Table 5
Real-time fluorescence quantitative PCR reaction system.

Composition	Volume
2 × SYBR Green	–
PCR mix	6.25 μl
Primer 1 (100 μM)	1 μl
Primer 2 (100 μM)	1 μl
Template DNA	2 μl
ddH2O	2.25 μl

Table 6
CDOCKER results of key target proteins and potential active compounds.

No.	Target	Interaction Energy - CIE (kJ·mol ⁻¹)	No.	Target	Interaction Energy - CIE (kJ·mol ⁻¹)
1	GRIN2B	60.8741	19	GRIN2B	59.8844
3	GRIA1	43.2904	20	GRIN2B	58.3027
4	BDNF	20.3176	20	BDNF	38.3721
5	CREB1	35.9604	22	NGF	24.3764
5	BDNF	34.4533	23	DLG4	42.3446
6	BDNF	37.254	25	GRIA1	65.0372
7	GRIA1	76.665	25	DLG4	45.7116
7	GRIN2B	71.5301	26	GRIA1	73.1775
9	GRIN2B	68.0292	26	GRIN2B	66.3009
9	DLG4	46.5057	26	DLG4	44.0477
9	BDNF	24.6209	27	DLG4	43.5068
10	BDNF	21.2997	28	GRIA1	67.1681
11	NGF	26.7186	30	GRIA1	89.769
12	NGF	20.0669	30	DLG4	46.3024
13	NGF	46.122	32	GRIA1	64.773
13	BDNF	36.567	32	DLG4	45.0812
14	NGF	26.7348	33	GRIA1	65.1203
15	BDNF	22.2057	36	BDNF	35.9596
16	NGF	31.9261	37	BDNF	22.6821
16	BDNF	20.7454	39	GRIA1	41.9827
17	BDNF	25.7357	39	GRIN2B	39.7152
18	GRIN2B	75.3036	40	GRIA1	42.856
18	GRIA1	64.3663	40	GRIN2B	31.2759
18	DLG4	45.8434	44	NGF	31.3481
18	BDNF	33.0618	44	BDNF	30.0307

Note: Compounds 2, 8, 21, 24, 29, 31, 34, 35, 38, 41, 42, 43 had poor docking results or no docking results and are not shown in the table. CIE represents CDOCKER_INTERACTION_ENERGY.

Table 7
Flexible docking results of key target proteins and 32 potential active compounds.

No.	Target	Interaction Energy - CIE (kJ·mol ⁻¹)	No.	Target	Interaction Energy - CIE (kJ·mol ⁻¹)
3	GRIA1	50.3581	14	NGF	26.98
4	BDNF	27.2565	22	GRIA1	34.7855
5	GRIN2B	57.3884	22	NGF	27.045
5	GRIA1	49.2758	39	GRIN2B	60.1676
10	GRIA1	38.4571	39	GRIA1	57.9125
11	GRIA1	32.1265	40	GRIN2B	63.1727
12	GRIA1	24.0778	40	GRIA1	50.01
12	NGF	22.0541	44	NGF	33.4617
13	GRIA1	57.9038			

Note: CIE represents CDOCKER_INTERACTION_ENERGY.

Compound 5 is *Curcumin*. Relevant studies have shown that *Curcumin* can regulate the expression levels of proteins related to synapsis and synaptic plasticity et cetera by promoting the regeneration of hippocampal neurons [51,52]. Compounds 39 and 40 are *Withaferin A* and *Withanolide A*, which are derived from *Withania somnifera*. Relevant studies have shown that the active components of *Withania somnifera* can prevent neurodegeneration, cognitive decline and synaptic plasticity damage, improve working memory, learning and motor coordination [47]. The flexible docking results showed that the three compounds all had high activity for GRIN2B and GRIA1. Many experimental studies have preliminarily confirmed the effect of *Curcumin* in anti-AD treatment [53,54]; therefore, our subsequent experiments will focus on *Withaferin A* and *Withanolide A*.

3.2. Pharmacokinetics prediction

The ADMET pharmacokinetics predictions of 12 compounds and the anti-AD drugs approved by the FDA were further analyzed to obtain their patent drug potential (Table 8). A total of 12 compounds could pass through the blood–brain barrier and reach specific areas of the brain to play their functional roles, of which compound 14 had the strongest blood–brain barrier penetration. A total of 12 compounds had good human intestinal absorption properties (HIA level was 0) and water solubility, and could be easily absorbed by the human body. Compounds 5, 14, 39, 40 and 44 did not show evidence of hepatotoxicity. Based on the analysis of the binding modes and the ADMET pharmacokinetics prediction of the compounds, we found that Compound 39 *Withaferin A* and Compound 40 *Withanolide A* had better binding modes and better pharmacokinetics properties, which were similar to the anti-AD drugs approved by the FDA for marketing (except for Rivastigmine, which had hepatotoxicity). Therefore, we conducted further pharmacological experiments on these compounds.

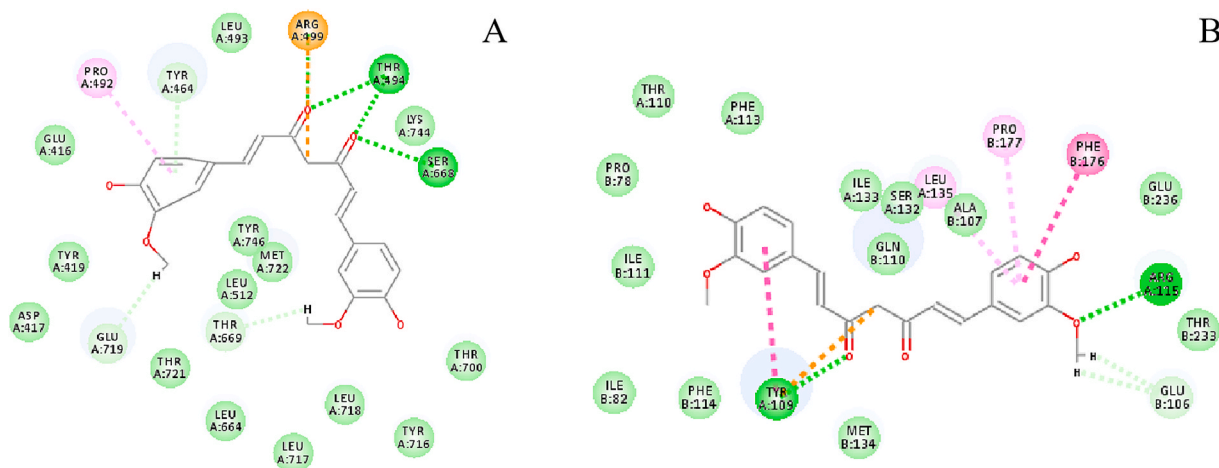


Fig. 1. Presumptive binding modes of Compound 5 and GRIN2B and GRIA1. (A) Compound 5 and GRIN2B. (B) Compound 5 and GRIA1. The dotted lines indicate the interactions between the compound and amino acid residues. Pink is hydrophobic interactions, green is hydrogen bond interactions, and tan is electrostatic interactions.

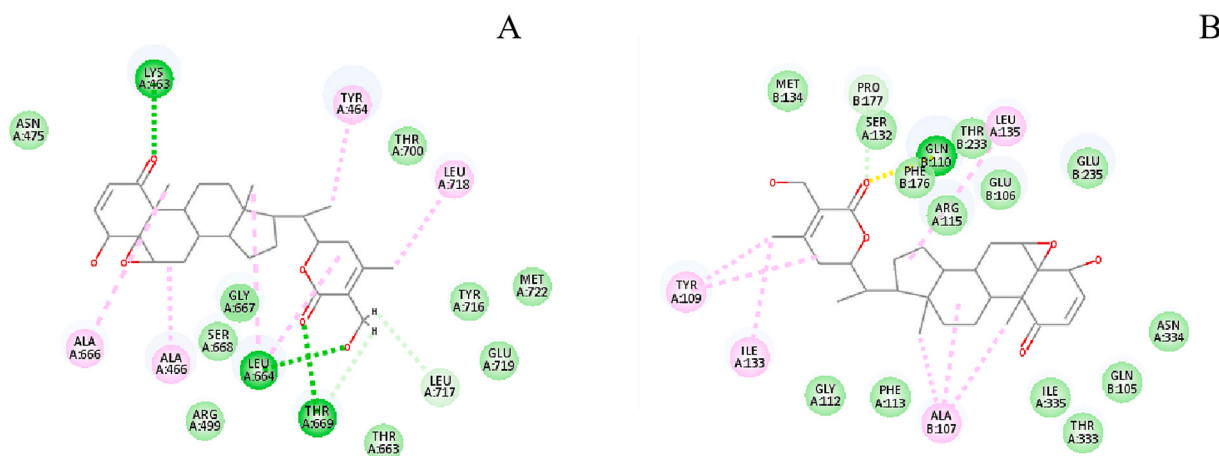


Fig. 2. Presumptive binding modes of Compound 39 and GRIN2B and GRIA1. (A) Compound 39 and GRIN2B. (B) Compound 39 and GRIA1. The dotted lines indicate the interactions between the compound and amino acid residues. Pink is hydrophobic interactions, green is hydrogen bond interactions, and tan is electrostatic interactions.

3.3. Biological experimental validation

3.3.1. Effects of different concentrations of H_2O_2 on the survival rate of hippocampal neurons

An MTT assay was used to detect the cell survival rate. The results showed that H_2O_2 treatment induced a marked decrease in cell viability by causing oxidative stress damage to neurons. Compared with the control group, the cell survival rates of the H_2O_2 (100 μ M, 150 μ M, 200 μ M, 250 μ M and 300 μ M) treatment groups were approximately 70%, 45%, 33%, 13% and 8%, respectively. When the H_2O_2 concentration was 150 μ M ($P < 0.001$) and damaged cells for 24 h, the cell survival rate was 50% ~ 60%, indicating the optimal injury model (Fig. 4).

3.3.2. In vitro toxicity test

An MTT assay was used to quantify the cell survival rate. The influences of different concentrations of *Withaferin A* and *Withanolide A* on the cell survival rate were compared with the control group to determine whether they were cytotoxic. Compared with the control group, when the concentration of *Withaferin A* reached 1 μ M, the cell viability was still approximately 94% (Fig. 5A), and when the concentration of *Withanolide A* reached 10 μ g/ml, the cell viability was approximately 88% (Fig. 5B). These results demonstrate that *Withaferin A* and *Withanolide A* were non-toxic to neurons ($P > 0.05$) within the range of the experimental concentrations.

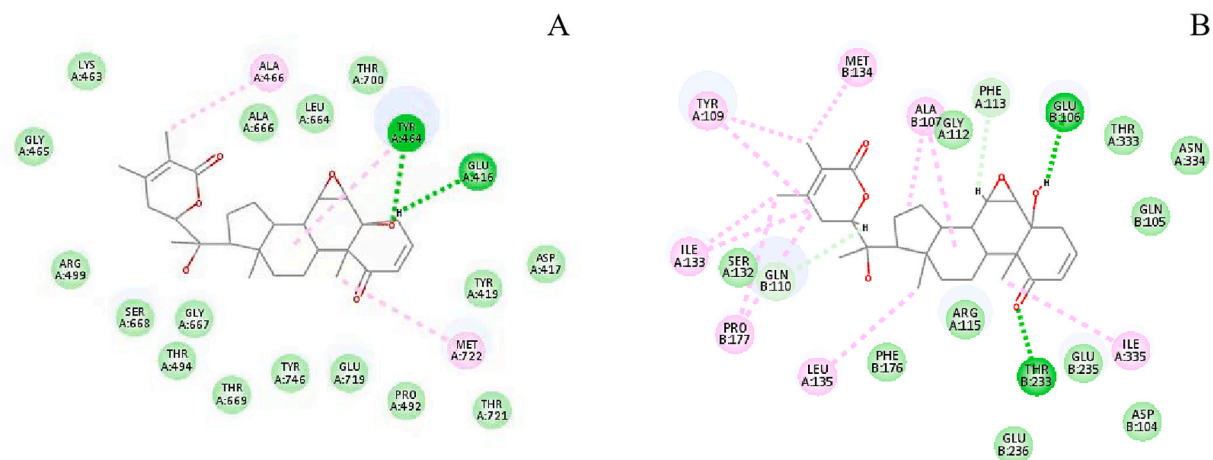


Fig. 3. Presumptive binding modes of Compound 40 and GRIN2B and GRIA1. (A) Compound 40 and GRIN2B. (B) Compound 40 and GRIA1. The dotted lines indicate the interactions between the compound and amino acid residues. Pink is hydrophobic interactions, green is hydrogen bond interactions, and tan is electrostatic interactions.

Table 8

Prediction of the ADMET properties.

No./Anti-AD Drugs	Blood Brain Barrier Penetration ^a	Human Intestinal Absorption ^b	Aqueous Solubility ^c	Hepatotoxicity ^d	Cytochrome P450 2D6 Inhibition ^e
3	3	0	3	-2.5142	-6.2602
4	3	0	3	-2.59951	-4.9925
5	3	0	3	-6.08138	-4.34328
10	3	0	3	0.622986	0.850929
11	2	0	3	0.738809	-1.26033
12	2	0	4	-0.937185	-5.21336
13	2	0	3	-3.01787	-3.06955
14	1	0	3	-5.87835	3.72647
22	3	0	3	0.158627	-3.75215
39	3	0	2	-5.1657	-4.55585
40	3	0	2	-6.64049	-2.95734
44	3	0	4	-4.70413	-4.19915
Donepezil	1	0	2	-29.133	-0.385985
Galantamine	2	0	3	-9.398	-2.6043
Rivastigmine	1	0	3	-1.37555	-1.89298
Memantine	1	0	3	-7.00437	-3.93433
Amantadine	2	0	3	-8.29128	-5.7308

Note: The anti-AD drugs (Donepezil, Galantamine, Rivastigmine, Memantine and Amantadine) information was inquired from U.S. Food and Drug Administration (fda.gov).

^a Blood Brain Barrier Penetration: 0-Super high; 1-High; 2-Medium; 3-Low; 4-Super low.

^b Human Intestinal Absorption: 0-Very good; 1-Good; 2-Medium; 3-Low.

^c Aqueous Solubility: 0 - No solubility; 1 - Super low; 2 - Medium; 3 - Good; 4 - Very good.

^d Hepatotoxicity: Value < -3, No hepatotoxicity; -3 < Value, Has hepatotoxicity.

^e Cytochrome P450 2D6 inhibition: Value < 0, No inhibition; 0 < Value, Has inhibition.

3.3.3. Withaferin A and withanolide A attenuate H₂O₂-induced neurotoxicity in hippocampal neurons

An MTT assay was used to detect the cell survival rate after drug intervention for 24 h. The neuroprotective effects of *Withaferin A* and *Withanolide A* against H₂O₂-induced toxicity were first examined in cultured suckling rat hippocampal neurons. The results showed that *Withaferin A* attenuated the H₂O₂-induced toxicity. When the concentration of *Withaferin A* was 0.5 μM, the cell viability was highest, at approximately 86% ($P < 0.001$) (Fig. 6A). There was no significant difference in the effects of different concentrations of *Withanolide A* on cell viability compared with the model group ($P > 0.05$). The cell viabilities were all between 50% and 60% (Fig. 6B). Therefore, *Withaferin A* had strong oxidation resistance and anti-AD potential, while the protective effect of *Withanolide A* on neurons was not obvious, and its anti-AD effect needs to be further verified.

3.3.4. Real-time fluorescence quantitative PCR detection of the downstream gene expression of key target proteins

To further explore the anti-AD mechanism, real-time fluorescence quantitative PCR (qPCR) was used to detect the effects of *Withaferin A* on the expression levels of the downstream genes BDNF, TrkB, CREB and ERK after binding with the key target proteins

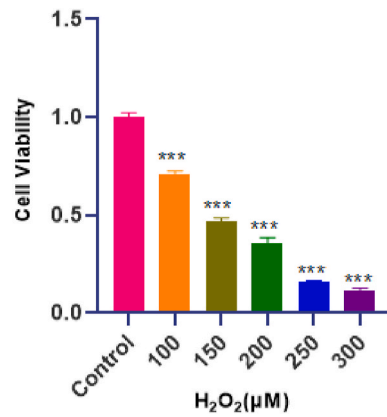


Fig. 4. Different neuron viabilities in different concentrations of H₂O₂. (***P* < 0.001).

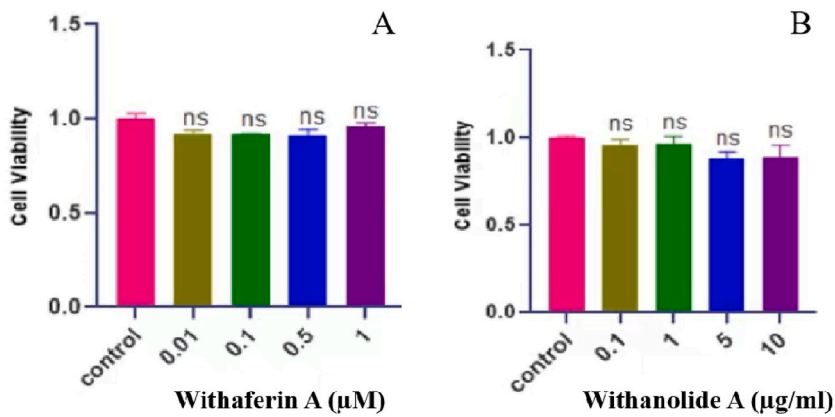


Fig. 5. Cytotoxicity of *Withaferin A* (A) and *Withanolide A* (B) to hippocampal neurons.

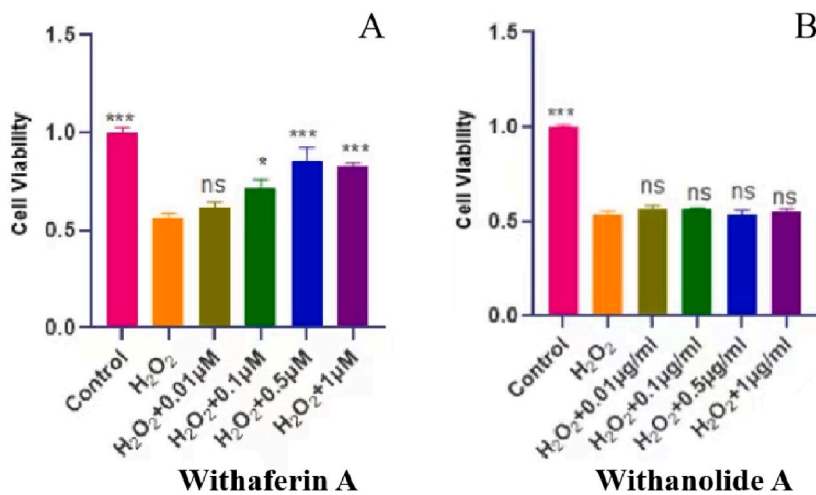


Fig. 6. Cell viability effect of *Withaferin A* (A) and *Withanolide A* (B) in the AD neurons model induced by H₂O₂. (**P* < 0.05, ****P* < 0.001).

GRIA1 and GRIN2B. BDNF, TrkB, CREB and ERK gene expression levels were significantly reduced after H₂O₂ damage (*P* < 0.01) (Fig. 7). After 24 h of 0.5 μM *Withaferin A* pretreatment, there was no significant difference in the expression levels of the BDNF, TrkB and ERK genes compared with the model group (*P* > 0.05) (Fig. 7A, B, D), but the expression of the CREB gene increased significantly

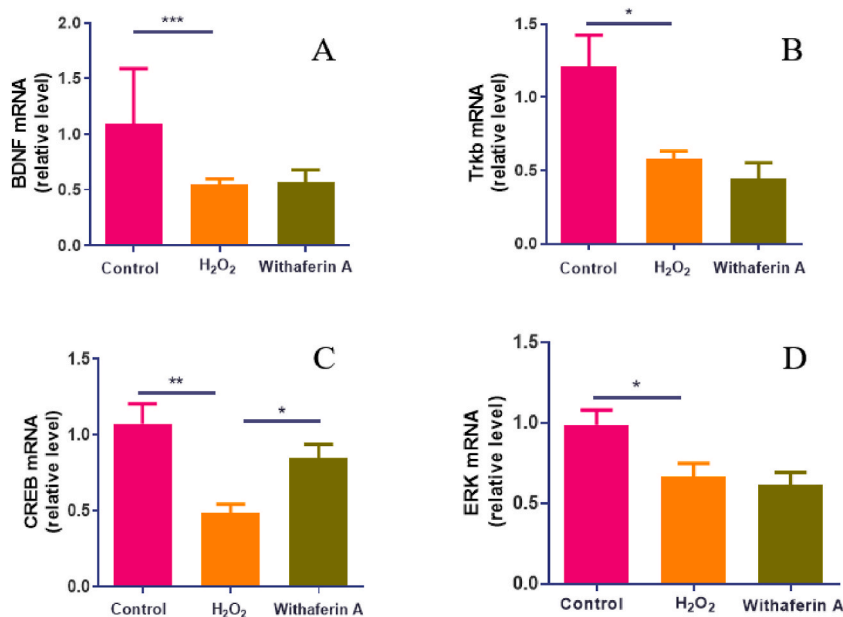


Fig. 7. Real-time fluorescence quantitative PCR to detect the effects of *Withaferin A* on the expression of the target genes BDNF (A), Trkb(B), CREB (C), ERK(D). (* $P < 0.05$, ** $P < 0.01$, *** $P < 0.001$).

($P < 0.05$) (Fig. 7C). These results showed that *Withaferin A* can protect neurons damaged by H_2O_2 by upregulating CREB. *Withaferin A* may activate pathways related to learning and memory function by upregulating CREB gene expression, subsequently enhancing cognitive function.

4. Discussion

In this study, *Withaferin A* was preliminarily determined as a lead compound anti-AD drug. *Withaferin A* is a steroid lactone isolated from the *Solanaceae* plant *Withania somnifera*. It is the main active ingredient extracted from the leaves, buds and roots of the *Withania somnifera*, which has been used as a medicinal plant in the Ayurvedic medical system in India for more than 3000 years. Studies have also confirmed that it shows good neuroprotective effects in neurological problems such as cognitive impairment and nerve injury. Due to its good curative efficacy in the treatment of nervous system, tumours and other diseases, it has attracted increasing amounts of attention from experts and scholars. However, most of the previous studies were conducted in the form of compound mixtures (e.g., *Withania somnifera* root extract). Therefore, which compound plays a direct role in AD is currently unknown, but with the deepening of the research, it was later found that *Withaferin A* may play a leading role in AD [55].

Oxidative stress plays a critical role in neuronal injury and is associated with various neurological diseases. It is believed to be one of the main causes of neurodegenerative diseases such as AD. The pathogenesis of AD is still not elucidated clearly but oxidative stress is one of the key hypotheses. Related studies showed that oxidative stress is a driving force for synapse dysfunction [56–58]. *Withaferin A* is a natural drug with neuroprotective effects, such as anti-inflammatory and antioxidation effects. Numerous studies have confirmed that *Withaferin A* shows strong anti-AD potential in different aspects. Tohda C [59] suggested that the methanol extract of *Withania somnifera* root has the activity to promote nerve axonal growth, mainly due to its active ingredient *Withaferin A*. Atluri V [60]'s study showed that *Withaferin A* significantly inhibited the production of $A\beta$ and the gene expression of neuroinflammatory molecules related to NF- κ B. In this study, we further verified that *Withaferin A* can protect the hippocampal neuron damaged by H_2O_2 , possessed oxidation resistance and no cytotoxicity.

Fully flexible molecular docking showed that *Withaferin A* has significant binding activity with the NMDA receptor subunit GRIN2B, and the interaction energy was $60.1676 \text{ kJ mol}^{-1}$. Real-time fluorescence quantitative PCR revealed that *Withaferin A* upregulated CREB gene expression. Related studies have shown that CREB has an important role in regulating synaptic plasticity and nerve regeneration. It can influence cognition by regulating the expression and interaction of synaptic plasticity-related genes [61] and is a key carrier for cell survival and cognition [62]. Translation mediated by CREB can promote the generation of synaptic connections, reduce the mortality of neurons and enhance cognitive function after brain injury [63]. In the central nervous system, the target protein CREB plays an important role in regulating neurons growth and synaptic plasticity. It participates in the formation of a molecular converter for the transformation from short-to long-term memory [64]. Because CREB plays important roles in memory formation and synaptic plasticity regulation, its dysfunction or decreased activity may lead to the development of cognitive impairment and neurodegenerative diseases [65].

Finally, we speculate that *Withaferin A* may upregulate the expression of the CREB gene through a downstream pathway mediated by the NMDA receptor subunit GRIN2B to regulate synaptic plasticity, activate the pathways related to learning and memory function

and promote the formation of long-term memory, and then play an anti-AD functional role. Therefore, enhancing CREB expression may be a potential therapeutic option [66].

5. Conclusion

In this study, DS 2019 was used to perform molecular docking on 7 key target proteins and 44 compounds with potential to enhance synaptic plasticity. A total of 12 active compounds had good binding effects with key target proteins, and ADMET prediction indicated that these compounds had greater possibility of becoming drugs. Among them, *Curcumin*, *Withaferin A* and *Withanolide A* had better binding stability with key target proteins and had good pharmacokinetic properties and multi-target potential. We carried out biological experimental validation experiments on *Withaferin A* and *Withanolide A*, and the MTT results showed that the protective effects of different concentrations of *Withanolide A* on neurons were not obvious. However, *Withaferin A* could inhibit H₂O₂-induced neuronal injury and effectively improve the cell survival rate. Through real-time fluorescent quantitative PCR detection, it was found that after *Withaferin A* pretreatment for 24 h, the expression of the CREB gene increased significantly. These results suggested that *Withaferin A* can play a protective role against H₂O₂-injured cells by upregulating CREB. Therefore, *Withaferin A* has potential as a lead compound in the development of a drug for Alzheimer's disease treatment on the basis of synaptic plasticity.

Author contribution statement

Heyu Wang: Conceived and designed the experiments; Analyzed and interpreted the data; Wrote the paper.

Quan Tang: Conceived and designed the experiments.

Yanyu Xue: Contributed reagents, materials, analysis tools or data.

Xiaoqian Gao: Analyzed and interpreted the data.

Yan Zhang: Analyzed and interpreted the data; Contributed reagents, materials, analysis tools or data; Wrote the paper.

Data availability statement

Data included in article/supplementary material/referenced in article.

Declaration of competing interest

The authors declare that they have no known competing financial interests or personal relationships that could have appeared to influence the work reported in this paper.

Acknowledgements

The authors thank the National Natural Science Foundation of China (No. 82071676).

References

- [1] E. Sügis, et al., HENA, heterogeneous network based data set for Alzheimer's disease, *Sci. Data* 6 (2019) 1–18.
- [2] C.S.B. Singh, et al., Reversing pathology in a preclinical model of Alzheimer's disease by hacking cerebrovascular neoangiogenesis with advanced cancer therapeutics, *EBioMedicine* 71 (2021) 1–14.
- [3] X.L. Liu, et al., Research progress on the mechanism of beta Amyloid protein in Alzheimer's disease, *Chin. J. Anat.* 43 (2020) 60–63.
- [4] D.L. Bi, et al., Development of potential therapeutic targets of and approaches to Alzheimer disease, *Chin. J. Pharmacol. Toxicol.* 29 (2015) 507–536.
- [5] Y.Y. Chen, et al., The role of inflammation-related factors in the pathogenesis of vascular dementia, *Chin. J. Biochem. Mol. Biol.* 35 (2019) 693–699.
- [6] Y. Chen, Neuronal synaptic plasticity, learning and memory, *Prog. Biochem. Biophys.* 35 (2008) 610–619.
- [7] F. Ding, *Neurobiology*, Science Press, China, 2012.
- [8] X.Y. Yan, A Study of the Tyrosine Phosphatase Sph2 Regulating the Tyrosine Phosphorylation of NMDAR and Synaptic Plasticity, 2015.
- [9] I. Mahar, Phenotypic alterations in hippocampal NPY- and PV-expressing interneurons in a presymptomatic transgenic mouse model of alzheimer's disease, *Front. Aging Neurosci.* 8 (2017) 1–12.
- [10] L. Wang, et al., Research progress on the pathogenesis of Alzheimer's disease, *Chin. J. Gerontol.* 37 (2017) 4953–4954.
- [11] L.A. Craig, et al., Revisiting the cholinergic hypothesis in the development of Alzheimer's disease, *Neurosci. Biobehav. Rev.* 35 (2011) 1397–1409.
- [12] H.Y. Liu, et al., Overview of the pathogenesis of Alzheimer's disease, *Geriatr. Health Care* 26 (2020) 1098–1100.
- [13] E. Tonnie, et al., Oxidative stress, synaptic dysfunction, and alzheimer's disease, *J. Alzheim. Dis.* 57 (2017) 1105–1121.
- [14] P. Mecocci, et al., A long journey into aging, brain aging, and alzheimer's disease following the oxidative stress tracks, *J. Alzheim. Dis.* 62 (2018) 1319–1335.
- [15] N. Lin, et al., Triphlorolide improves age-associated cognitive deficits by reversing hippocampal synaptic plasticity impairment and NMDA receptor dysfunction in SAMP8 mice, *Behav. Brain Res.* 258 (2014) 8–18.
- [16] L. Wei, et al., Pratensein attenuates A β -induced cognitive deficits in rats: enhancement of synaptic plasticity and cholinergic function, *Fitoterapia* 101 (2015) 208–217.
- [17] P. Liu, et al., Effects and mechanism of Xanthoceraside on synaptic plasticity in APP/PS1 transgenic mice, *Acta. Neuropharmacologica.* 8 (2018) 32.
- [18] J.-i. Kim, et al., Platycodon grandiflorus root extract improves learning and memory by enhancing synaptogenesis in mice Hippocampus, *Nutrients* 9 (2017) 1–15.
- [19] Y.W. LingHu, et al., Advances in the research of Lycoris, *Subtrop. Plant. Sci.* 36 (2007) 73–76.
- [20] Y. Liu, et al., Research progress on chemical constituents and structure-activity relationship of alkaloids from plants of Lycoris herb, *Forestry and Environmental Science* 35 (2019) 114–121.
- [21] Y.Y. Xue, et al., Exploring the mechanism of anti-alzheimer's disease based on the theory of synaptic plasticity, *Journal of MUC (Natural Sciences Edition)* 30 (2021) 23–33.

- [22] X.H. Ma, et al., Neuroprotective effect of paeoniflorin on okadaic acid-induced tau hyperphosphorylation via calpain/Akt/GSK-3 β pathway in SH-SY5Y cells, *Brain Res.* 1690 (2018) 1–11.
- [23] Y.J. Xu, et al., Albiflorin ameliorates memory deficits in APP/PS1 transgenic mice via ameliorating mitochondrial dysfunction, *Brain Res.* 1719 (2019) 113–123.
- [24] Y. Wang, et al., Huperzine A alleviates synaptic deficits and modulates amyloidogenic and nonamyloidogenic pathways in APPswe/PS1dE9 transgenic mice, *J. Neurosci. Res.* 90 (2012) 508–517.
- [25] C. Vivar, Adult hippocampal neurogenesis, aging and neurodegenerative diseases: possible strategies to prevent cognitive impairment, *Curr. Trends Med. Chem.* 15 (2015) 2175–2192.
- [26] J. Liang, et al., Dihydropyridinone ameliorates behavioral deficits and reverses neuropathology of transgenic mouse models of alzheimer's disease, *Neurochem. Res.* 39 (2014) 1171–1181.
- [27] J. Wang, et al., Epigenetic modulation of inflammation and synaptic plasticity promotes resilience against stress in mice, *Nat. Commun.* 9 (2018) 1–14.
- [28] D.S. Rivera, et al., Andrographolide recovers cognitive impairment in a natural model of Alzheimer's disease (*Octodon degus*), *Neurobiol. Aging* 46 (2016) 204–220.
- [29] M.M.H. Bhuiyan, et al., Radix Puerariae modulates glutamatergic synaptic architecture and potentiates functional synaptic plasticity in primary hippocampal neurons, *J. Ethnopharmacol.* 209 (2017) 100–107.
- [30] A. Sarkaki, et al., Chrysin prevents cognitive and hippocampal long-term potentiation deficits and inflammation in rat with cerebral hypoperfusion and reperfusion injury, *Life Sci.* 226 (2019) 202–209.
- [31] X.L. Zhu, et al., Novel antidepressant effects of Paeonol alleviate neuronal injury with concomitant alterations in BDNF, Rac1 and RhoA levels in chronic unpredictable mild stress rats, *Psychopharmacology* 235 (2018) 2177–2191.
- [32] Y. Hirshler, et al., Neuroplasticity-related mechanisms underlying the antidepressant-like effects of traditional herbal medicines, *Eur. Neuropsychopharmacol* 27 (2017) 945–958.
- [33] B. Hughes, et al., Cannabidiol reverses deficits in hippocampal LTP in a model of alzheimer's disease, *Neurochem. Res.* 44 (2019) 703–713.
- [34] Z.H. Yao, et al., Luteolin could improve cognitive dysfunction by inhibiting neuroinflammation, *Neurochem. Res.* 43 (2018) 806–820.
- [35] P.J. Wei, et al., Tenuigenin enhances hippocampal Schaffer collateral-CA1 synaptic transmission through modulating intracellular calcium, *Phytomedicine* 22 (2015) 807–812.
- [36] C. Sheng, et al., Icarin attenuates synaptic and cognitive deficits in an $\text{A}\beta_{1-42}$ -induced rat model of alzheimer's disease, *BioMed Res. Int.* 2017 (2017) 1–12.
- [37] E. Joseph, et al., Neuroprotective effects of apocynin and galantamine during the chronic administration of scopolamine in an alzheimer's disease model, *J. Mol. Neurosci.* 70 (2020) 180–193.
- [38] L. Li, et al., Multi-target strategy and experimental studies of traditional Chinese medicine for alzheimer's disease therapy, *Curr. Trends Med. Chem.* 16 (2016) 537–548.
- [39] X.Y. Qin, et al., Progress in the research on chemical constituents and pharmacological activities of coeloglossum, *Journal of MUC (Natural Sciences Edition)* 16 (2007) 229–232.
- [40] X.X. Du, et al., Research progress of three ginsenoside monomers against alzheimer's disease, *West China, J. Pharmaceut. Sci.* 33 (2018) 323–327.
- [41] K. Radad, et al., Ginsenosides and their CNS targets, *CNS Neurosci. Ther.* 17 (2011) 761–768.
- [42] E. Suzuki, et al., The facilitative effects of bilobalide, a unique constituent of Ginkgo biloba, on synaptic transmission and plasticity in hippocampal subfields, *J. Physiol. Sci.* 61 (2011) 421–427.
- [43] C. Montecinos-Oliva, et al., Effects of tetrahydrohyperforin in mouse hippocampal slices: neuroprotection, long-term potentiation and TRPC channels, *Curr. Med. Chem.* 21 (2014) 3494–3506.
- [44] A. Khan, et al., Neuroprotective effect of quercetin against the detrimental effects of LPS in the adult mouse brain, *Front. Pharmacol.* 9 (2018) 1–16.
- [45] M.V. Turovskaya, et al., Taxifolin protects neurons against ischemic injury in vitro via the activation of antioxidant systems and signal transduction pathways of GABAergic neurons, *Mol. Cell. Neurosci.* 96 (2019) 10–24.
- [46] K. Wang, et al., Oleonic acid ameliorates $\text{A}\beta_{25-35}$ injection-induced memory deficit in alzheimer's disease model rats by maintaining synaptic plasticity, *CNS Neurol. Disord. - Drug Targets* 17 (2018) 389–399.
- [47] M. Gupta, et al., Withania somnifera (L.) Dunal ameliorates neurodegeneration and cognitive impairments associated with systemic inflammation, *BMC Compl. Alternative Med.* 19 (2019) 1–18.
- [48] K. Sudarshan, et al., Discovery of an isocoumarin analogue that modulates neuronal functions via neurotrophin receptor TrkB, *Bioorg. Med. Chem. Lett.* 29 (2019) 585–590.
- [49] S. Patel, et al., Cytisine halts the advance of Alzheimer's disease-like pathology and associated depressive-like behavior in Tg6799 mice, *Front. Aging Neurosci.* 6 (2014) 1–13.
- [50] C. Nie, et al., Betaine reverses the memory impairments in a chronic cerebral hypoperfusion rat model, *Neurosci. Lett.* 615 (2016) 9–14.
- [51] S.J. Kim, et al., Curcumin stimulates proliferation of embryonic neural progenitor cells and neurogenesis in the adult Hippocampus, *J. Biol. Chem.* 283 (2008) 14497–14505.
- [52] S.A. Frautschy, et al., Phenolic anti-inflammatory antioxidant reversal of A β -induced cognitive deficits and neuropathology, *Neurobiol. Aging* 22 (2001) 993–1005.
- [53] C. Vivar, Adult hippocampal neurogenesis, aging and neurodegenerative diseases: possible strategies to prevent cognitive impairment, *Curr. Trends Med. Chem.* 15 (2015) 2175–2192.
- [54] S. Samarghandian, et al., Anti-oxidative effects of curcumin on immobilization-induced oxidative stress in rat brain, liver and kidney, *Biomed. Pharmacother.* 87 (2017) 223–229.
- [55] N. Tian, et al., Roles of withaferin compounds in nervous system disorders, *Chin. Pharmacol. Bull.* 35 (2019) 4–7.
- [56] P.K. Kamat, et al., Mechanism of oxidative stress and synapse dysfunction in the pathogenesis of alzheimer's disease: understanding the therapeutics strategies, *Mol. Neurobiol.* 53 (2016) 648–661.
- [57] T. Scheuer, et al., Neonatal oxidative stress impairs cortical synapse formation and GABA homeostasis in parvalbumin-expressing interneurons, *Oxid. Med. Cell. Longev.* (2022) 1–12.
- [58] A. Fesharaki-Zadeh, et al., Oxidative stress in traumatic brain injury, *Int. J. Mol. Sci.* 23 (2022) 1–19.
- [59] C. Tohda, New age therapy for alzheimer's disease by neuronal network reconstruction, *Biol. Pharm. Bull.* 39 (2016) 1569–1575.
- [60] V.S.R. Atluri, et al., Inhibition of amyloid-beta production, associated neuroinflammation, and histone deacetylase 2-mediated epigenetic modifications prevent neuropathology in alzheimer's disease in vitro model, *Front. Aging Neurosci.* 11 (2020) 1–11.
- [61] E. Benito, et al., CREB's control of intrinsic and synaptic plasticity: implications for CREB-dependent memory models, *Trends Neurosci.* 33 (2010) 230–240.
- [62] X. Yang, et al., Influence of learning and memory on the expression of relevant controlling protein PDE-4 and extracellular signal regulating kinase, *Med. Recapitulate* 17 (2011) 2241–2243.
- [63] D. Li, et al., Icarin: a potential promoting compound for cartilage tissue engineering, *Osteoarthritis Cartilage* 20 (2012) 1647–1656.
- [64] X.Y. Chen, et al., CREB and alzheimer's disease, *Chin. J. Neuroimmunol. Neurol.* 15 (2008) 144–148.
- [65] M. Xie, NR2B Mediated Effects of Dysfunction of Ubiquitin-Proteasome System Components on CREB Activity, 2014.
- [66] R.S. Bitner, Cyclic AMP response element-binding protein (CREB) phosphorylation: a mechanistic marker in the development of memory enhancing Alzheimer's disease therapeutics, *Biochem. Pharmacol.* 83 (2012) 705–714.